sustainability

MDPI

Article

Seismic Performance and Failure Mechanisms of Reinforced Concrete Structures Subject to the Earthquakes in Türkiye

Ercan Işık [1], Fatih Avcil [1,*], Marijana Hadzima-Nyarko [2,*], Rabia İzol [3], Aydın Büyüksaraç [4], Enes Arkan [5], Dorin Radu [6] and Zeki Özcan [7]

[1] Department of Civil Engineering, Bitlis Eren University, Bitlis 13100, Türkiye; eisik@beu.edu.tr
[2] Department of Civil Engineering, Josip Juraj Strossmayer University of Osijek, Vladimira Preloga 3, 31000 Osijek, Croatia
[3] Department of Civil Engineering, Middle East Technical University, Ankara 06100, Türkiye; rizol@metu.edu.tr
[4] Vocational School, Çanakkale 18 Mart University, Çanakkale 17400, Türkiye; absarac@comu.edu.tr
[5] Department of Architecture, Bitlis Eren University, Bitlis 13100, Türkiye; earkan@beu.edu.tr
[6] Faculty of Civil Engineering, Transilvania University of Brașov, 500152 Brașov, Romania; dorin.radu@unitbv.ro
[7] Department of Civil Engineering, Sakarya University, Sakarya 54100, Türkiye; ozcan@sakarya.edu.tr
* Correspondence: favcil@beu.edu.tr (F.A.); mhadzima@gfos.hr (M.H.-N.)

Abstract: Many reinforced-concrete structures collapsed or were seriously damaged in the 7.7 and 7.6 magnitude earthquakes that occurred in southern Türkiye on 6 February 2023. The recorded peak ground accelerations were quite high (2.2 g) and the recorded motions' elastic acceleration response spectra were significantly greater than the elastic design spectra given by the most recent Turkish seismic design code. A total of 518,000 houses were heavily damaged or collapsed in the eleven cities affected by the earthquake. More than 53,000 people lost their lives and over 100,000 people were injured, the majority of these injurits caused by the collapse of reinforced concrete structures. Post-earthquake damage assessments are important in the context of applying sustainability principles to building design and construction. In this study, post-earthquake damage assesments and evaluations were made for the reinforced-concrete structures that were exposed to destruction or various structural damage in Hatay, Kahramanmaraş and Adıyaman, which where most affected after the Kahramanmaraş earthquakes. The RC building damage and failure mechanisms resulting from field observations were evaluated in detail from a broad performance-based structural and earthquake engineering perspective. Information about Kahramanmaraş earthquakes is given briefly. Design spectra and spectral accelerations were compared for the earthquake stations in these three provinces. Soft/weak story, short column, insufficiently reinforced-concrete, and poor workmanship are the primary causes of structural damage, which cause earthquake weaknesses in these buildings.

Keywords: Kahramanmaraş; earthquake; reinforced concrete; failure mechanism

Citation: Işık, E.; Avcil, F.; Hadzima-Nyarko, M.; İzol, R.; Büyüksaraç, A.; Arkan, E.; Radu, D.; Özcan, Z. Seismic Performance and Failure Mechanisms of Reinforced Concrete Structures Subject to the Earthquakes in Türkiye. *Sustainability* **2024**, *16*, 6473. https://doi.org/10.3390/su16156473

Academic Editor: Maged A. Youssef

Received: 10 July 2024
Revised: 26 July 2024
Accepted: 27 July 2024
Published: 29 July 2024

1. Introduction

Damage assessment after any natural disaster is important in order to minimize the impact of the disaster and increase resilience to possible disasters. In this context, evaluation of post-earthquake damages within the framework of cause–effect plays a critical role in making both new and existing buildings more resistant to earthquakes. Damage data enable urban planning and infrastructure design to be used within the scope of sustainability to reduce earthquake risk. All kinds of damage data can be used towards sustainability principles for the reconstruction process in the destroyed environment after the earthquake and the development of earthquake-resistant building design principles. These data can enable the production of economically sustainable solutions in the long term. Education and awareness campaigns using structural damage data enable people to understand earthquake risks and take precautions. It is necessary to know the

effects of earthquakes on structures in detail in order to increase earthquake resistance and sustainable earthquake management.

Earthquakes can affect a wide range of areas and cause varying levels of damage to different types of structures. The effects of earthquakes on structures may vary depending on the characteristics of the earthquakes, local ground conditions and structural features. Research on these features and their interaction after earthquakes in different parts of the world has a significant importance in terms of earthquake and civil engineering. Earthquakes can cause much greater damage to the overall environment, especially in high seismic risk regions. In this study, the impact of the very destructive earthquakes that recently occurred in Türkiye, which is located in the Alpine–Himalayan earthquake zone with high seismic risk, was taken into account.

Türkiye, as a country, is located in one of the highest seismically active zones of the world. The 2011 Van (M_w = 7.2), 2020 Elazığ (M_w = 6.8), 2020 İzmir (M_w = 6.6), and 2022 Düzce (M_w = 6.0) earthquakes that occurred in the last 20 years reveal the continuity of seismic activity. Finally, on the Eastern Anatolian Fault (EAF), where no significant earthquake activity has been experienced for a long time, two different and independent earthquakes, their epicenters in Pazarcık and Elbistan (M_w = 7.7 and M_w = 7.6, respectively) districts of Kahramanmaraş city, occurred on the same day and caused great destruction. Earthquakes caused the death of many people and great economic loss in a very large region covering the provinces of Şanlıurfa, Osmaniye, Malatya, Kilis, Kahramanmaraş, Diyarbakır, Gaziantep, Hatay, Elazığ, Adana, and Adıyaman. Among these provinces, the three most affected were Hatay, Kahramanmaraş, and Adıyaman. As a consequence of the disasters, more than 50,000 people lost their lives and approximately 38,000 buildings were destroyed. Besides this damage to buildings, other engineering structures, such as airports, highways, railways, bridges, industrial facilities, power lines, drinking water and wastewater, infrastructure facilities, etc. were also damaged. During these earthquakes, events such as landslides, lateral spreading, rock falls, and liquefaction were also commonly observed in the region.

It is estimated that the total cost of earthquakes for the Turkish economy is approximately 104 billion dollars. It is also estimated that this size corresponds to approximately 9% of the national income for 2023 [1]. It has been stated that 55% of this is due to housing damage, 13% to the destruction in public infrastructure and service buildings, and 13% to private sector damage excluding housing [1]. Among the earthquakes that occurred in Türkiye this century, these were the largest in terms of human and economic losses. Determining building damage after an earthquake is significant in terms of continuing social life, determining the earthquake hazard for specific settlements, and developing codes regarding structures. The data to be collected are very valuable for the development of civil and earthquake engineering after earthquakes. Damage evaluations to be made during this process should be completed as quickly and practically as possible. There are many studies evaluating post-earthquake structural damage in this way [2–7]. In this study, observational damage assessments and evaluations were made for reinforced concrete (RC) buildings by the authors in the earthquake region. These and related post-earthquake studies are all regarded as case studies that have the potential to significantly impact academia and practice. Many studies have been conducted after each earthquake in various parts of the world regarding the effects of earthquakes on structures. Arslan and Korkmaz [8] studied the effects of disasters in Türkiye on reinforced concrete structures within the scope of the earthquake regulations used in the country. Furtado et al. [9] examined the seismic behavior of reinforced concrete structures with infill walls in light of current earthquakes. Maeda et al. (2012) [10] investigated the structural failures that occurred in reinforced concrete structures after the 2011 Eastern Japan earthquakes. Kaplan et al. [11] evaluated the damage in reinforced concrete and masonry structures as a result of their field observations following the 2009 L'Aquila (Italy) earthquakes. Işık et al. [12] evaluated the damage to reinforced concrete structures after the 2011 Van earthquake and made an example web-based application for determination of damage. Kaplan et al. [13] examined the post-earthquake

of the 2003 Bingöl (Türkiye) damages to reinforced concrete buildings. Arslan [14] tried to determine the main design parameters affecting the earthquake performance of reinforced concrete buildings with artificial neural networks. Ruiz-Pinilla et al. [15] revealed the lessons to be learned from the damage to reinforced concrete structures after the 2011 Spain earthquake. Braga et al. [16] evaluated the damage to non-structural elements in reinforced concrete structures after the 2009 Italian earthquake. Valente and Milani [17] made reinforcement recommendations to increase the earthquake performance of reinforced concrete buildings. Masi et al. [18] evaluated the damage occurring to structural and non-structural members in reinforced concrete structures after the 2016 Italy earthquake. Damcı et al. [19] evaluated the structural damage in buildings with different structural systems after the 2011 Van earthquake. Çağlar et al. [20] evaluated the damage assessments resulting from the 2020 Elazığ earthquake as a result of field observations.

There are also some studies proposing various methods for rapid seismic performance evaluation, such as the use of machine learning, the use of equivalent single-degree-of-freedom models with capacity curves, and the probability matrix method. Won and Shin [21] studied the framework for creating an artificial neural network-based model that can quickly forecast seismic reactions with the effects of soil–structure interaction and identify the seismic performance levels. Xu et al. [22] studied a methodology for assessing seismic damage to reinforced concrete buildings using computer vision and machine learning. Xiong et al. [23] carried out parameter determination and damage evaluation for THA-based damage estimation of multi-story structures in China during the 2014 Ludian earthquake. Tian et al. [24] recommend a framework for cost–benefit assessments that consider seismic risk, seismic damage, retrofit costs, economic losses, and cost–benefit analyses for city-scale seismic retrofitting of structures. Leggieri et al. [25] studied the geographic information system (GIS) to propose a technique for the extraction, integration, and elaboration of data from various sources to create a georeferenced building database (GBD) that is helpful in the large-scale seismic vulnerability assessment of existing buildings. Erduran [26] examined the hysteretic energy demands in multi-degree-of-freedom systems subjected to earthquakes. Gentile and Galasso [27] proposed metamodels that map engineering demand parameters using ground motion intensity measures. Fajfar [28] presented a simplified analysis of the seismic performance of structures by combining the pushover analysis of a multi-degree-of-freedom model with the response spectrum analysis of an equivalent single-degree-of-freedom system. Harirchian et al. [29] used five different machine learning approaches to classify earthquake damage for four different earthquakes.

Many studies have found their place in the literature on the evaluation of the damage to structures with various structural systems after the 6 February 2023 Kahramanmaraş earthquakes, which caused severe damage in 11 different provinces and directly affected more than 14 million people. Işık et al. [30] evaluated the failure of the mosques and minarets in Adıyaman province. Ivanov and Chow [31] made damage assessments in RC buildings in Adıyaman City after the Pazarcık and Elbistan earthquakes and stated that material properties are an important factor. Kahya et al. [32] examined the post-earthquake damage to masonry structures in Hatay province within the framework of cause and effect. Avcil [33] and Arslan et al. [34] evaluated prefabricated structures damaged in the earthquake region within the framework of field observations and structural analyses. Işık [35] examined in detail mud-brick structures damaged at different levels in the earthquake zone. Karaşin [36] investigated the impacts of the two Kahramanmaraş earthquakes in Diyarbakır city. Zengin and Aydın [37] studied the impact of material quality on damage in moderately and heavily damaged reinforced concrete structures. İnce [38] studied the impacts of both earthquakes on RC structures in Adıyaman city. Ozturk et al. [39] examined the influences of earthquakes on school buildings. Ozturk et al. [40] worked in detail on the failures in reinforced concrete buildings within the scope of earthquake regulations. Akar et al. [41] evaluated the damage incurred to different structural systems in Gölbaşı, one of the districts where local ground conditions have the greatest impact on buildings. Binici et al. [42] studied the damage to reinforced concrete, in Gaziantep, Hatay, Kahramanmaraş,

Adana and Adyıman provinces, based on observation. Işık et al. [43] comparatively examined target displacement values as well as damage assessments for reinforced concrete buildings in Adıyaman province. Çetin et al. [44] especially examined soil liquefaction and its consequences in the provinces affected by these earthquakes. Kocaman et al. [45] tried to reveal the effects of earthquakes in the case of Malatya Yeni Mosque with the help of numerical models. Kocaman [46] examined the damage to historical masonry mosques and minarets and numerically demonstrated the earthquake behavior of the Adıyaman Grand Mosque. Mercimek [47] examined in detail the failure damage to masonry buildings in the earthquake region. Tunç et al. [48] investigated the effects of the recent Sivrice–İzmir and Kahramanmaraş earthquakes in Türkiye on buildings. Ersöz et al. [49] conducted a study on rapid damage assessment in these earthquakes with the help of digital technologies. Kazaz et al. [50] examined the seismic behavior of the structures that were especially heavily damaged after theses earthquakes. Nemutlu et al. [51] compared the losses occurring in earthquakes with estimated values. Each of these can be considered as a case study allowing a more realistic understanding of the earthquake–structure interaction. Within the scope of this study, R/C structures in Kahramanmaraş, Hatay and Adıyaman, the three provinces most affected by earthquakes, were taken into consideration.

In this study, as a result of the field observations carried out by the authors, the structural damage to the R/C structures in Hatay, Adıyaman, and Kahramanmaraş, the three cities most affected by the disaster, were evaluated. Structural damage examples resulting from field investigations were evaluated comparatively, taking into account the conditions given in the earthquake regulations. For each example of damage, structures located in different settlements were taken into account. Information regarding the earthquakes on 6 February 2023, was also provided by the study. The impacts of the two earthquakes, which caused great destruction, on the R/C buildings in the earthquake zone were investigated within the scope of earthquake and civil engineering. Recommendations were made taking into account all the results obtained. The primary characteristic that sets this study apart from others is the examination of structural damage in the three provinces most affected by the earthquake. Each damage condition is also shown schematically. This study can be a source for similar studies, and contribute to the measures that can be taken in the development and implementation of earthquake regulations.

2. 6 February 2023 Kahramanmaraş (Türkiye) Earthquakes

Examining Türkiye's tectonic system reveals that Eastern Anatolia is compressed, as the Arabian Plate, which is a portion of the African Plate, pushes northward to meet the Eurasian Plate. The Anatolian Plate is seen to be moving westward due to this compression, by the effect of the North Anatolian Fault Zone (NAFZ), and the East Anatolian Fault (EAF) (Figure 1). EAF has a length of approximately 580 km, and several earthquakes have occurred along its length, making it one of Türkiye's highest seismically active regions. Major earthquakes of the instrumental period that occurred in fault zones are illustrated in Figure 2 on the current earthquake hazard map used in Türkiye. The Anatolian plate's southeast boundary is formed by the left-lateral strike–slip EAF and destructive earthquakes happen along these faults, which intersect the NAFZ in Karlıova [52,53]. Similarly, the Dead Sea Fault Zone (DSFZ) and the EAF combine at Antakya. Conversely, it essentially stretches in seven distinct portions southwestward from Karlıova to Iskenderun Bay [54,55]. This region has experienced catastrophic earthquakes for almost two millennia, according to historical and instrumental data [56–61]. Major earthquakes that occurred in the historical period in EAF were the 1114 ($M > 7.8$) and 1513 ($M > 7.4$) Maraş Earthquakes, the 1822 Halep Earthquake ($M_S = 7.5$), the 1866 Bingöl Earthquake ($M_S = 7.2$), 1872 Amik Lake earthquake ($M_S = 7.2$), 1874 ($M_S = 7.1$) and 1875 ($M_S = 6.7$) Hazar Lake earthquakes and 1893 Malatya Earthquake ($M_S = 7.1$) [62]. In the instrumental period, the 1905 Malatya earthquake ($M_S = 6.8$), the 1966 Varto earthquake ($M_S = 6.2$), the 1971 Bingöl earthquake ($M_S = 6.8$), the 2003 Tunceli earthquake ($M_d = 6.1$), 2010 ($M_L = 5.8$) and the 2020 ($M_w = 6.8$) Elazığ earthquakes occurred, but these earthquakes were not as devastating as the historical

earthquakes. According to Çetin et al. [63], the fault locked during this period caused the seismic quiescence along the whole EAF. The NE end of the EAF is where historical earthquakes begin and continue toward the SW. The center and southwest regions of the EAF are primarily responsible for the distribution of past earthquakes. For the past 500 years, there has not been a catastrophic earthquake that might induce a surface rupture on the Gölbaşı–Türkoğlu stretch, where the fault folds into the SW.

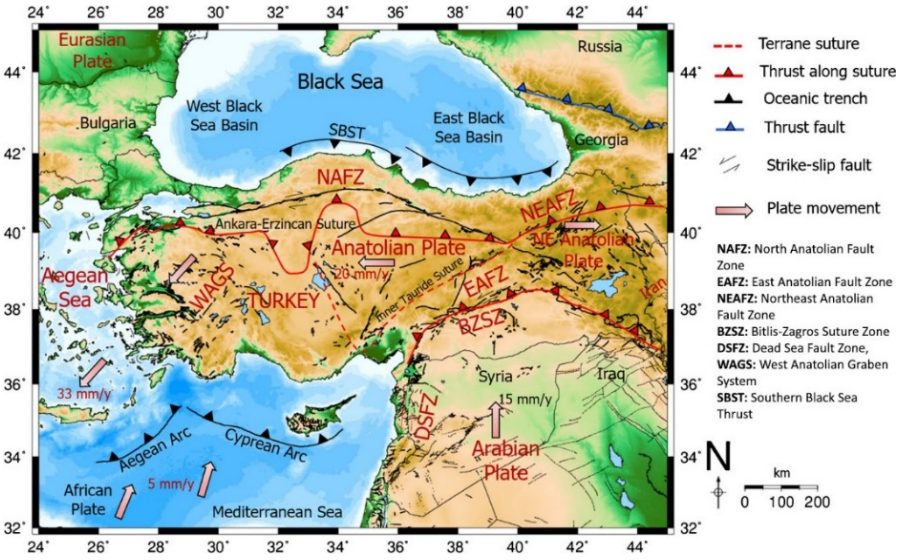

Figure 1. Tectonic map of Türkiye and surroundings [64].

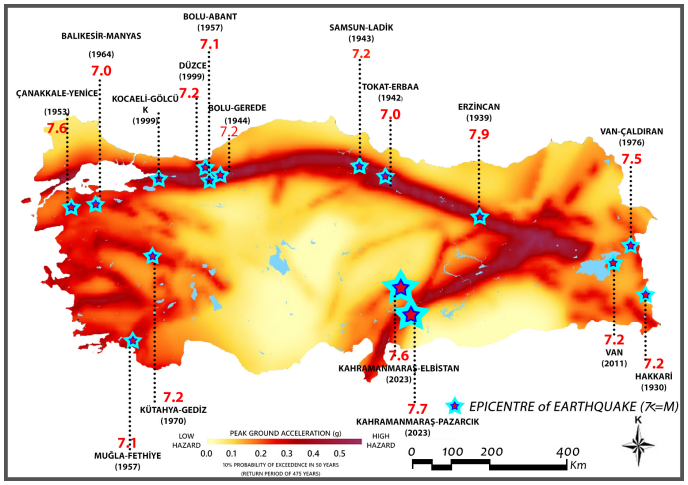

Figure 2. Major earthquakes occurring in Türkiye (adopted from [65]).

Türkiye, which is located in a very high-risk geographical area in terms of seismicity, has been affected by major earthquakes that have caused great destruction throughout the historical process. Earthquakes with a magnitude greater than 7 in the country are shown in Figure 2.

According to GPS research, the EAF is sliding 9–10 mm annually [66–68]. Following bifurcation, the northern shore shares around one-third of this activity [54,69–71]. According to Over et al. [72], the last significant earthquake to strike this area happened in 1872 and had an acceleration of about 0.4 g. Numerous academics concur that an earthquake was predicted by pointing out a seismic gap in this area following the prior earthquakes along the EAF and the Sivrice (Elazığ) earthquake (M_w = 6.8) in 2020 [73,74].

On 6 February 2023, at 04:17 and 13:24 Türkiye time, two independent and very devastating seismic events of magnitude M_w = 7.7 and M_w = 7.6 occurred, with epicenters in the Pazarcık and Elbistan district of Kahramanmaraş. While the depth of the initial earthquake was 8.6 km, the depth of the subsequent earthquake was 7 km and both earthquakes were very close to the surface. While the aftershock activity of these two independent earthquake pairs continued, another "triggered" earthquake with a magnitude of M_w = 6.4 occurred in Yayladağı (Hatay) on 20 February 2023. Unlike other earthquakes that occurred in the country, both earthquakes had significant effects on a very wide region. The earthquakes were felt very strongly and caused loss of life and heavy damage in 11 different cities, especially Kahramanmaraş, Adıyaman, and Hatay cities, as well as Elazığ, Şanlıurfa, Osmaniye, Adana, Diyarbakır, Kilis, Gaziantep, and Malatya. These 11 different settlements affected by the earthquake are shown on the map in Figure 3.

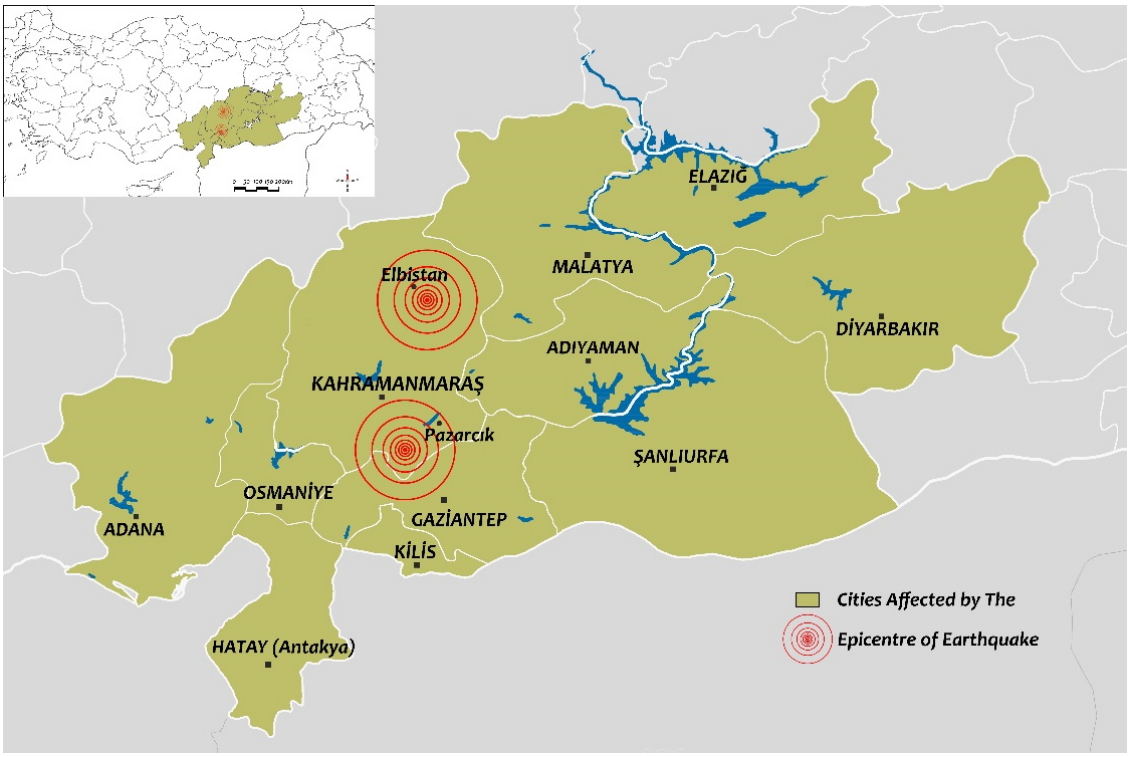

Figure 3. The epicenter of two earthquake couples and the borders of the affected area.

The moment magnitude, depth, and moment tensor solution of these earthquakes are summarized in Table 1 as reported by the Minister of Interior, Disaster and Emergency Management Presidency (AFAD) [75]. Following the characteristics of the EAF, the fault mechanism of the first earthquake was a left-lateral strike–slip. The second earthquake, the M_w = 7.6 Elbistan earthquake, which occurred approximately 9 h later, created a surface rupture along the Çardak–Sürgü fault section. It was identified south of Elbistan and near Ekinözü. Similar to the first earthquake, the moment tensor solution of this disaster indicates a right-lateral strike–slip motion. In the earthquake that occurred further south on February 20, normal faulting was observed. Focal mechanism solutions of 149 aftershocks were made by Büyüksaraç et al. [76] and it was revealed that the fault plane solutions of the aftershocks showed predominantly strike–slip mechanisms in response to the nearly N–S and E–W oriented left lateral strike–slip mechanisms of the DSFZ and EAF.

Table 1. Moment tensor solutions of earthquakes [75].

Beach Ball	M_w	Strike 1	Dip 1	Rake 1	Strike 2	Dip 2	Rake 2
	7.7	233	74	18	140	77	168
	7.6	358	73	174	90	86	13
	6.4	214	57	−44	332	55	−138

Acceleration-time graphs of the stations with peak ground acceleration (PGA) values for the provinces of Adıyaman (0201 station), Hatay (3129 station), and Kahramanmaraş (4614) in the first earthquake, whose epicenter was at Pazarcık, are shown in Figure 4. E–W, N–S, and U–D acceleration spectra and the representation according to different probabilities of exceedance are shown in Figure 5. Comparisons were made taking into account four different earthquake ground motion levels currently specified in the seismic design code in Türkiye. While the largest earthquake with a recurrence period of 2475 is expressed as DD-1, the standard design ground motion level with a recurrence period of 475 is expressed as DD-2. The remaining two earthquakes are called frequent and service earthquakes with ground motion levels and are shown as DD-3 and DD-4. In this study, the design spectrum obtained for DD-1 and DD-2 was used in comparisons. Among the horizontal acceleration values of the station, the E–W component exceeded the DD-1 and DD-2 design acceleration spectrum values, and N–S exceeded the DD-2 design acceleration spectrum value. Likewise, vertical acceleration spectrum values exceeded DD-2 design acceleration values. Spectrum acceleration values of both horizontal and vertical acceleration records at stations 4614 and 3129 exceeded the DD-1 and DD-2 design acceleration and the spectrum values.

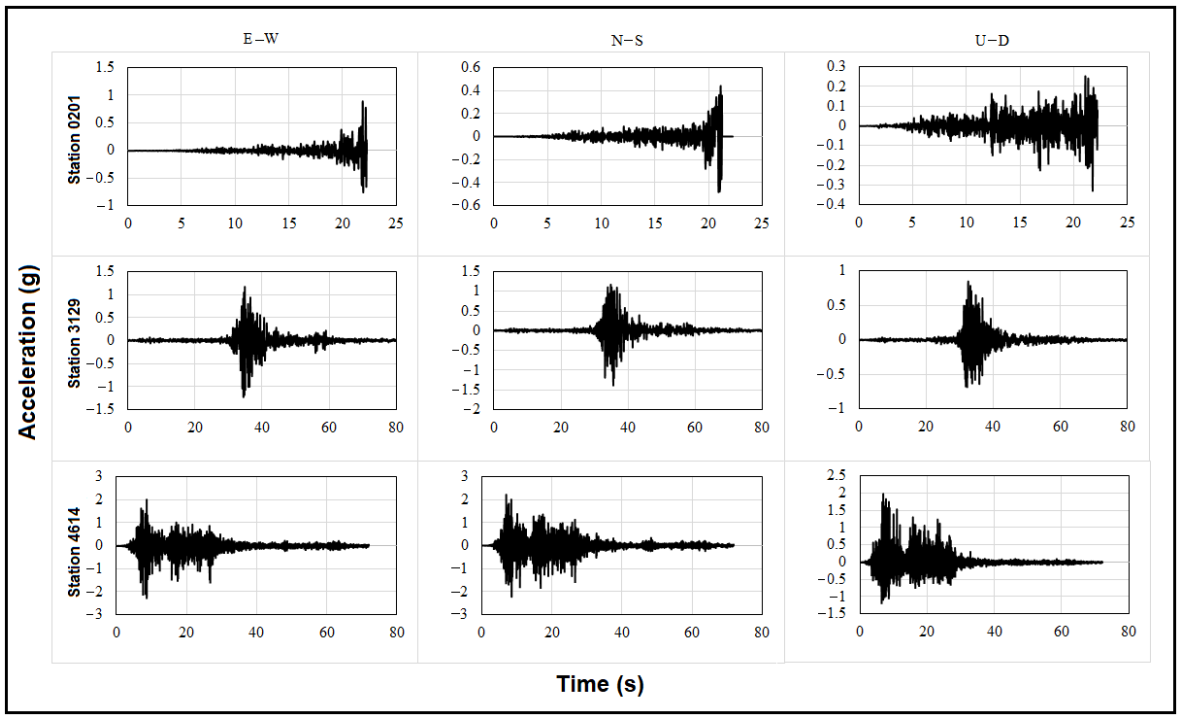

Figure 4. Components of recorded ground accelerations of the Pazarcık earthquake.

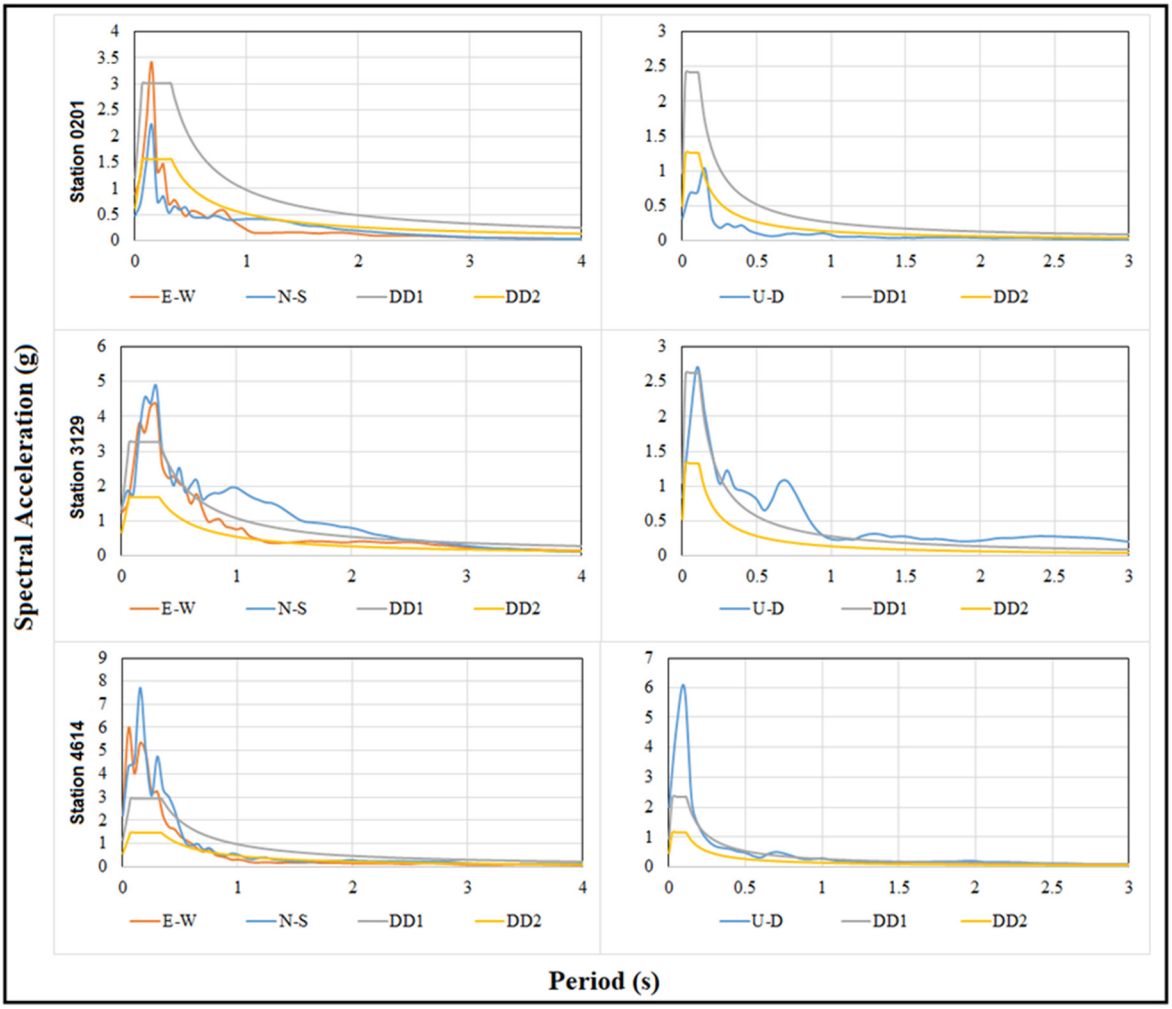

Figure 5. Design spectrums and spectral accelerations of three acceleration stations installed in Kahramanmaraş, Hatay, and Adıyaman.

3. Damages in R/C Structures during the Destructive Earthquakes

Local soil conditions directly affected the earthquake performance and structural damage levels of buildings in the Kahramanmaraş earthquakes, like in other major earthquakes. As a result of field assessments, ground-related structural damage was frequently observed, especially in settlements such as the Gölbaşı district of Adıyaman province, Kahramanmaraş (Kuyumcular and Çiğli Village), Antakya and İskenderun. In addition, earthquake effects have been clearly observed on the ground surface in different ways. One of these has been lateral spreads that occurred in the ground surface. As a consequence of lateral spreading, cracks, steepness, and depressions occur. Some samples of lateral spreading are shown in Figure 6. Lateral spread towards a free face is seen in Figure 6a,c, whereas in Figure 6b,d lateral spread down gentle slopes is shown, where a free face is absent.

Liquefaction of the soil is the loss of its strength, hardness and solidity as a result of earthquake shaking or similar rapid and heavy loading. When the layers under the level of groundwater quickly become weaker and behave more like a viscous liquid than a solid, this is known as ground liquefaction. Liquefaction damage is shown in Figure 7.

Figure 6. Ground-related damage after the earthquakes; (**a**,**c**) lateral spread towards a free face; (**b**,**d**) lateral spread down gentle slopes.

Figure 7. Damage caused by liquefaction.

Foundation settlements and rotations may occur due to the bearing capacity of the soil, whose shear strength decreases due to liquefaction. As a result of these, structural damage may occur when structures on such soils rotate away from the foundation and overturn.

In Figure 8, such damage is displayed. Additionally, insufficient foundation depth and weak design of structure–soil interaction are other factors that contribute to such damages.

Figure 8. Examples of the lack of sufficient foundation depth.

Local soil conditions must be determined realistically by in situ geotechnical tests. In addition, soil–structure interaction must be taken into consideration realistically in building design. Foundation type, foundation width, length, and depth selections should be made accordingly. In addition, if the soil properties are very poor, ground reinforcement methods should also be considered. Necessary precautions should be taken, especially on the ground, where there is a risk of liquefaction. In addition, basement floors, which have a positive effect on the earthquake performance of the building, should be considered and implemented in building construction. In this context, the currently used Turkish Building Earthquake Regulation (TBEC-2018) [77] has paid special attention to this situation with very detailed and different sections regarding both local ground and foundations.

As a result of the difference in stiffness/strength between stories in a reinforced concrete building, a weak/soft story is formed. Soft story formation has been observed for many different reasons, such as changing the load-bearing system between stories or using different flooring systems between stories. Soft story irregularity is among the most important causes of building damage during earthquakes. This irregularity is included in almost every post-earthquake examination report. Although some stories of the buildings had completely collapsed, it can be seen that even the windows of the upper stories had not broken. Soft stories may occur due to the building load-bearing systems having different characteristics between floors (such as high story heights) or due to the change in the number of partition walls, which are not considered to belong to the load-bearing system. The collapses that occurred on the intermediate floors are shown in Figure 9.

Figure 9. Samples of weak story damage.

The cause of failure observed in most of the structures that were subjected to complete collapse in the earthquake zone was the soft story. In these buildings, especially those located on main streets, the ground floor is generally used as a commercial enterprise, while the upper floors are used for residential purposes. The amount of infill wall varies due to the change in purpose of use. In this case, complete collapse occurred as the upper floors of the building collapsed onto the soft story. Sample buildings that partially or totally collapsed and became unusable as a consequence of the soft ground story are shown in Figure 10.

Figure 10. Examples of buildings with partially or completely collapsed ground story due to soft stories.

In the last three earthquake codes used in Türkiye (1998, 2007, 2018), the strength and stiffness irregularity between adjacent floors has found its place under "Vertical Irregularity". There are no criteria regarding this situation in the 1975 Earthquake Regulations. The strength irregularity between adjacent stories (weak story) has not undergone any changes in the last three regulations. While the stiffness irregularity between adjacent floors (soft story) uses the same criteria in the last two earthquake codes and the limit value of the stiffness irregularity coefficient is specified as 2, this value is limited to 1.5 in the 1998 earthquake code. There are no criteria in the 1975 earthquake regulations.

Irregularities that create a weak or soft story mechanism in any story should be avoided. In this context, necessary precautions should be taken in the building load-bearing system to eliminate the negative effects of sudden stiffness and strength decreases caused by the removal of infill walls, which are not taken into account in the load-bearing system calculation but may have significant stiffness in their planes, on some floors and especially on the ground floors of buildings. Care should be taken not to change the purpose of use and height within the building.

The pancake-type collapse was the type of damage observed during the Kahramanmaraş earthquakes, which caused the total collapse of the structure and made search and rescue efforts under the rubble the most difficult. This situation causes the upper floors of the buildings to collapse on the lower floors in an earthquake. When buildings could not absorb the energy caused by the earthquake, they were subjected to complete collapse. Insufficiently reinforced concrete, not using reinforced concrete shear walls, not ensuring continuity between load-bearing elements, and creating strong beams and weak columns can be counted among the causes of such damage. Sample images for pancake collapse are shown in Figure 11.

Figure 11. Examples of pancake-type collapse.

To prevent such collapses, a sufficient amount of reinforced concrete shear walls should be used in both directions to increase the rigidity of the structure, the criteria given in the earthquake regulations should be complied with for the columns to be stronger than the beams, and the ductility and continuity of the structural system members that form the reinforced concrete frames should be ensured to be sufficient.

Another type of damage encountered in reinforced concrete structures after an earthquake is damage caused by short columns. Short column behavior is the brittle behavior of the reinforcing bars in the building element under the earthquake effect due to the shear force before reaching the yield level, causing collapse damage. Band windows, which are generally used in buildings, may produce short columns due to the change in column heights within the structure [78]. If the column net length (l_n) taken into account in the building design is smaller than the calculated value, the V_e shear force value increases, and. with the earthquake effect, more load is loaded than the V_e shear force value calculated for the column. In this case, short column damage is encountered. In cases where the formation of short columns cannot be prevented, the shear force is to be taken as the basis in the calculation of transverse reinforcement;

$$V_e = (M_{ru} + M_{rl})/l_n \quad (1)$$

In this equation, M_{rl} denotes the column lower-end moment and M_{ru} denotes the column upper-end moment. Bending moments will be calculated as $M_l \approx M_{rl}1.4$ and $M_u \approx 1.4\, M_{ru}$ at the lower and upper ends of the short column, ln will be taken as the free length of the short column and the calculated shear force must meet the conditions given below;

$$V_c \leq V_r \qquad V_c \leq 0.85\, A_w.\, f_{ck} \quad (2)$$

In short column design, minimum transverse reinforcement and placement conditions defined for confined boundary regions must be applied throughout the entire column. If the infill walls are completely adjacent to the columns, transverse reinforcement will be continued throughout the entire floor height for the columns that work as short columns (Figure 12).

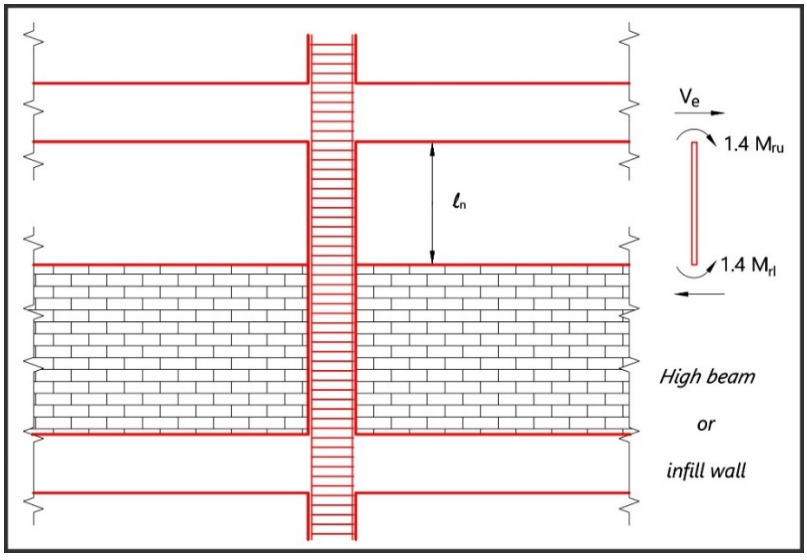

Figure 12. Transverse reinforcement in short column [77].

There are no rules or recommendations regarding the formation of short columns in the earthquake regulations of 1975. The same rules apply in the last three earthquake regulations, 1998, 2007, and 2018. The damages that occurred in the short columns created without complying with the above-mentioned conditions in the 6 February 2023 earthquake couple are shown in Figure 13.

Figure 13. Examples of short column damage.

Various levels of damage have also occurred in the infill walls used to delimit and separate spaces in reinforced concrete structures. In general, the low mechanical properties of wall materials, which are given an aesthetic appearance by using gypsum plaster without the use of lime–cement plaster, as well as poor masonry work, have negatively affected the structural damage occurring in these elements. Some examples of damage encountered in infill walls are shown in Figure 14. This damage was generally observed as shear cracks and out-of-plane failure.

Figure 14. Examples of infill wall damage because of the Kahramanmaraş earthquakes.

To prevent infill wall damage, rough plaster must be used and appropriate wall material and masonry must be provided. In addition, the mortar used on the walls must be applied in a way that provides sufficient interlocking. Failure to adequately clamp the

slabs used in reinforced concrete structures to the beam and column members to which they are connected, and failure to ensure full continuity between the elements, causes the slabs to separate from these structural members and be damaged. Samples of such failure are shown in Figure 15.

Figure 15. Damage caused by inadequate slab–beam–column connection.

The construction of shear walls in reinforced concrete structures without complying with earthquake-resistant structure design principles caused the load bearing capacity to be exceeded in these members and led to structural damage at different levels. In particular, failure to form shear wall boundary zones, excessive transverse reinforcement spacing, and use of low-strength concrete increased the extent of damage to wall elements. Examples of shear wall damage are shown in Figure 16.

Figure 16. RC shear wall damages.

The shear walls section and reinforcement detail in the currently used earthquake regulations are given in Figure 17.

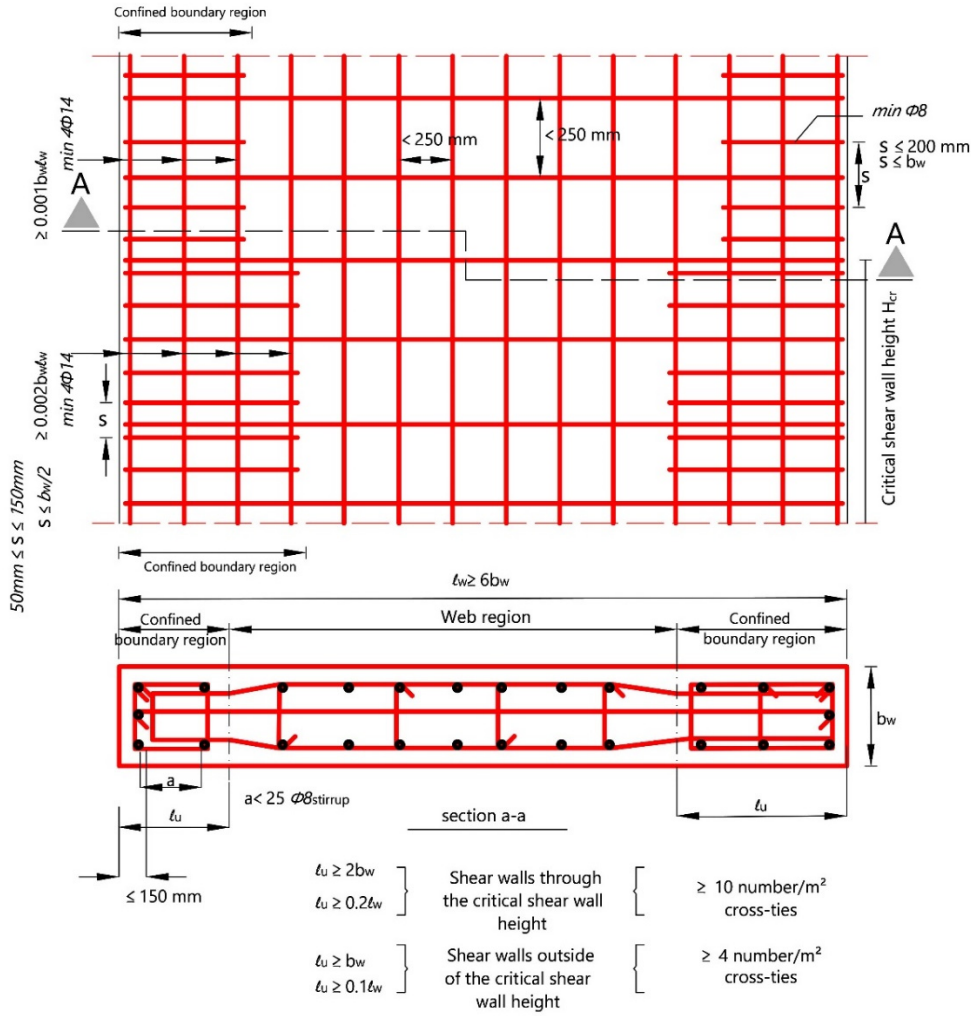

Figure 17. RC shear walls section and reinforcement detail [77].

During an earthquake, plastic hinges are desired to form in beams, not columns. In some buildings, beams have larger cross-sections, higher strength, and are more rigid than columns. This case causes the columns to be exposed to large shear forces, causing brittle failures, and then complete collapse may occur. Examples of plastic hinge damage occurring at the lower and upper-end points of the column are shown in Figures 18 and 19, respectively. Plastic hinge damages occurring at the upper ends of the column due to the cantilever beam effect are also illustrated in Figure 20.

In adjacent reinforced concrete structures without sufficient gap, additional shear forces occur in the neighboring structures due to the pounding effect. In this case, as a result of exceeding the shear force capacity of the RC columns, significant damage occurs at different levels in adjacent buildings. Structural damage caused by the pounding effect is illustrated in Figure 21.

Concrete cover, which is a part of the reinforced concrete structural element, is used to protect the reinforcement used in reinforced concrete bearing members from external effects. This section, not made of sufficient thickness, corrodes over time, causing both the bearing capacity to decrease and the cross-sectional area to decrease, causing crushing damage to the concrete in this area. Rusting and resulting structural damage due to insufficient concrete cover thickness are shown in Figure 22.

Figure 18. Examples of the plastic hinge damage at the lower end of the column.

Figure 19. Examples of the plastic hinge damage at the upper end of the column.

Figure 20. Examples of the plastic hinge damage due to the cantilever beam effect.

Figure 21. Structural failures caused by the pounding effect.

Figure 22. Examples of buildings with insufficient concrete cover.

One of the roles expected from transverse reinforcement is to reduce the brittle feature of the core concrete. Transverse reinforcements fulfill this function by confining the core concrete. Insufficient adherence between concrete with reinforcement and low-strength concrete caused the core concrete to be completely crushed. Examples of such structural damage are illustrated in Figure 23.

Figure 23. Structural failures caused by the crushing of core concrete in columns.

For the stirrups or cross-ties to be used in the columns to interlock for the longitudinal reinforcement, the connection must be made at an angle of 135°. This stipulation is necessary for adequate interlocking between transverse and longitudinal reinforcement. Otherwise, the transverse reinforcement will separate from the longitudinal reinforcement and have problems in performing its roles. This also negatively affects the adherence between transverse reinforcement and concrete. Damage caused by such misuse is shown in Figure 24.

Figure 24. Structural failures caused by application fault of stirrups.

The stirrups end commonly have 90° hooks and do not overlap in damaged columns in the earthquake region. It is specified that closed stirrups with 135° hooks are used, and the stirrups interlock into the core concrete in Turkish Standards. Correct and incorrect applications of the stirrup according to the Turkish standard are illustrated in Figure 25.

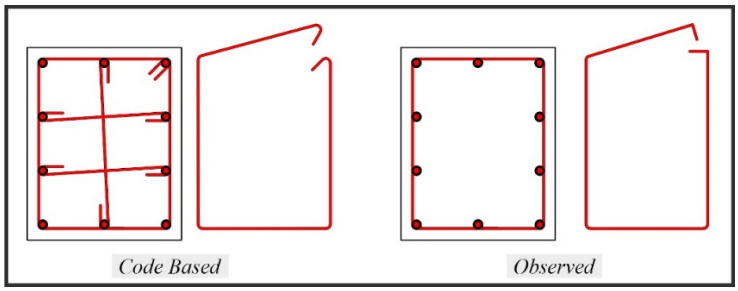

Figure 25. Correct and incorrect application of the stirrup.

Another cause of damage is crushing damage to the concrete as a result of not using sufficient reinforcement in the column–beam connection. Failure to pay due attention to

the embedment and addition of reinforcement, which was not used in sufficient quantities, caused damage in these areas, and examples of such failure are shown in Figure 26.

Figure 26. RC building damage caused by insufficient reinforcement in the column–beam joint.

A comparative representation of the transverse reinforcement conditions in columns and beams in the last two earthquake codes is shown in Figure 27.

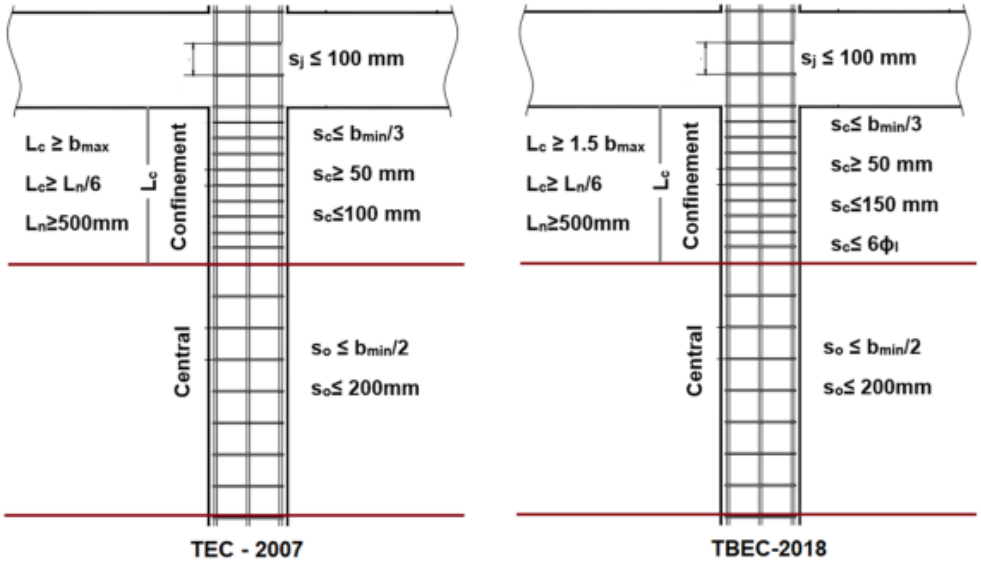

Figure 27. Comparison of the last two earthquake regulations in Türkiye [77,79].

Wooden roofs used in reinforced concrete structures and gable walls on the roofs are other parts that are damaged during earthquakes. Such observed failures are shown in Figure 28.

Inappropriate aggregate granulometry and usage of the stream aggregate directly affect the concrete strength in RC structures. The different levels of damage that occur in the structural elements due to improper aggregate grain distribution, placement of concrete, compaction, and lack of care during maintenance stages are shown in Figure 29. Failure to use appropriately sized aggregate negatively affects both the adherence of the aggregate within itself and the adherence to the reinforcement.

Figure 28. Samples of roof gable wall failure and collapsed roof.

Figure 29. Examples of structural damage resulting from improper aggregate granulometry.

The reinforcements used in many structures that were heavily damaged in the earthquake zone are plain reinforcements. Both the bearing capacity and the adherence between plain reinforcement and concrete are much lower than in ribbed reinforcement. Examples of damage resulting from this are shown in Figure 30.

Passing electrical and machinery-like installations through the load-bearing system members in buildings reduces the effective cross-sectional areas of these elements, causing significant losses in bearing capacity. Examples of installations passing through structural elements are shown in Figure 31.

The main function of stirrups or cross-ties used in reinforced concrete columns and beams is to resist the shear forces that occur. Reinforcement strength, diameter, spacing, and concrete strength directly affect the shear force capacity. In addition, there must be dimensional harmony between the longitudinal reinforcement diameter and the transverse reinforcement diameter. Otherwise, the transverse reinforcement may be separated from the longitudinal reinforcement and stripped. Examples of damage caused by inadequate transverse reinforcement are illustrated in Figure 32.

Figure 30. Examples of damaged structures using flat reinforcement.

Figure 31. Examples of installations passing through structural system elements.

Figure 32. Structural failures caused by insufficient transverse reinforcement.

In some R/C structures, heavy overhangs are built on the floors above the ground floor to increase the usage area. There have been parts of the commonly used heavy overhangs, that extend beyond the R/C frame, which were damaged during the earthquake. Samples of structural failure at different levels in heavy overhangs are illustrated in Figure 33.

Although many structures around them collapsed during the earthquake, many structures resist the earthquake and provide life safety performance levels. Some such buildings are shown in Figure 34.

Schematic representations of reinforced concrete structure failures are shown in Figure 35. Schematic representations of the types of damage encountered in the observations made in the earthquake area are also shown in Figure 36.

Figure 33. Examples of the structural damage caused by heavy overhangs.

Figure 34. Some buildings that provide life safety.

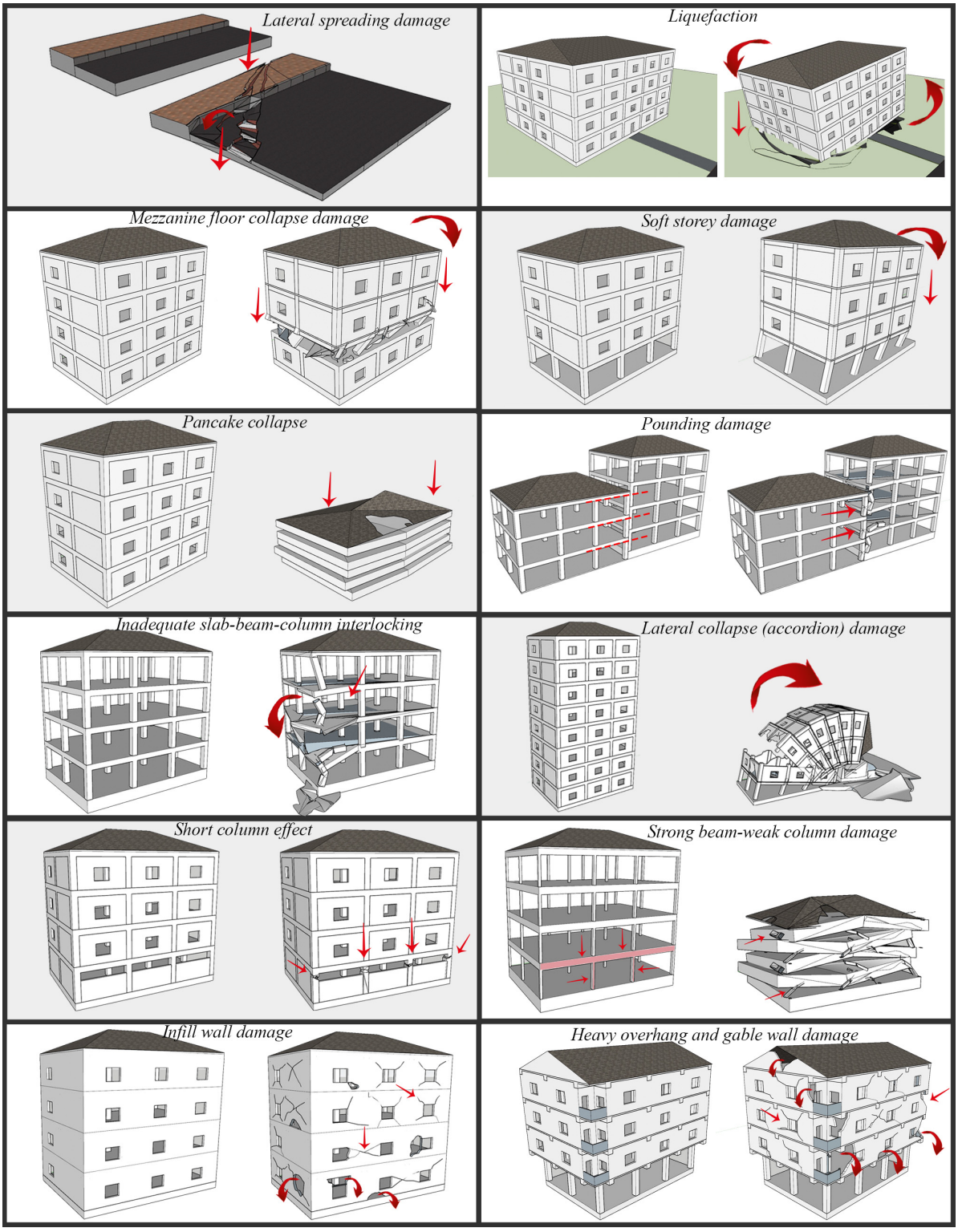

Figure 35. Representations of structural failure.

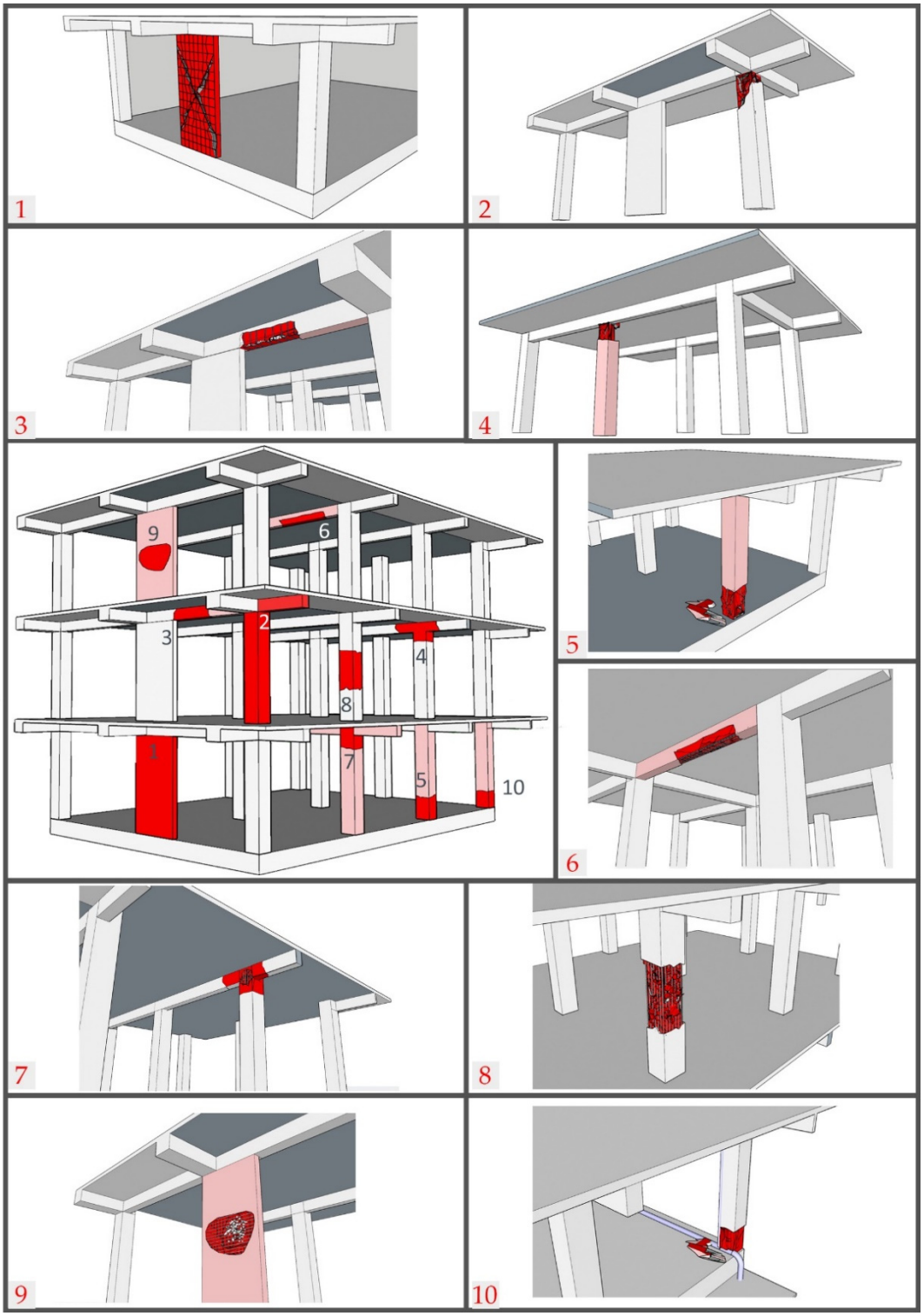

Figure 36. Schematic representation of damage. (1) RC shear wall. (2) Plastic hinge damages due to the cantilever beam effect. (3) Insufficient concrete cover and corrosion of reinforcement. (4) Plastic hinge damage occurring at the upper-end points of the column. (5) Plastic hinge damage occurring at the lower-end points of the column. (6) Insufficient transverse reinforcement. (7) Inadequate reinforcement details at the column–beam connection zones. (8) Low-strength of the concrete. (9) Improper aggregate granulometry. (10) Installations passing through structural system.

4. Results and Conclusions

The structural damage that occurred in reinforced concrete structures during the M_w = 7.7 and M_w = 7.6 magnitude earthquakes that occurred in Kahramanmaraş/Pazarcık and Kahramanmaraş/Elbistan on 6 February 2023 were examined in detail in the earthquake region immediately after the earthquake by the authors. In this study, damaged reinforced concrete structures in Hatay, Kahramanmaraş, and Adıyaman provinces, where earthquakes caused the most damage, the most deaths, and the greatest economic loss, were taken into consideration. The causes of damage to RC structures as a result of field observations are stated below;

- Using plain (non-ribbed) reinforcements
- Construction of heavy overhangs
- Effect of short columns
- Using low-strength concrete
- Improper aggregate granulometry
- Insufficient bond between concrete and reinforcement
- Insufficient transverse reinforcement
- Strength and rigidity differences between floors (Weak/soft story)
- RC structures built adjacent to each other (pounding effect)
- Inadequate concrete cover thickness
- Corrosion of reinforcement
- Embedment problem in transverse reinforcement
- Not using cross-ties
- RC shear walls not being constructed by earthquake-resistant building design principles
- Opening of stirrups causes buckling of the longitudinal bars under axial load and crushing and disintegration of core concrete.
- Poor infill masonry and not using rendering in these wall
- Heavy cantilever beams cause plastic hinges at the upper ends of the column
- Plastic hinges formed in columns before beams

The intensity characteristics observed at certain distances from faults caused by earthquakes vary significantly. These differences are thought to be related to the soil properties of structures and various construction issues, as well as to proximity to the fault and the characteristics of settlements in the basin area. Although the peak ground acceleration (PGA) and velocities (PGV) recorded by accelerometers in the region show less variability with respect to intensity values, they exhibit high values at distant locations. The goodness-of-fit coefficient for the best-fit curve of PGA and PGV values remains low due to the wide range of values. PGA acceleration values ranging from 400 cm/s^2 to 1000 cm/s^2 have been recorded up to 40 km from the fault, corresponding to intensity levels of VIII–IX. Many PGV values have been recorded up to 40 km from the fault, reaching a velocity of 200 cm/s. At distances up to 120 km from the fault, intensity values are concentrated between V and VII, and this area corresponds to PGA values ranging from 20 cm/s^2 to 400 cm/s^2. Additionally, PGV values corresponding to intensity IX, ranging from 90 cm/s to 200 cm/s, have been observed up to 20 km from the fault.

Following the devastating earthquakes of 6 February 2023 in Kahramanmaraş, Türkiye, extensive geotechnical and structural evaluations were conducted across affected regions, particularly in Hatay, Kahramanmaraş, and Adıyaman. This study investigated the damage to reinforced concrete structures, considering factors such as structural failure mechanisms, local site conditions, and strong ground motion characteristics. Key findings are summarized below:

The vulnerability of structures in Antakya, Türkoğlu, and Gölbaşı was exacerbated by their location on former riverbeds and lakebeds, characterized by soft soil deposits. These conditions led to significant seismic amplification, magnifying ground motion, and increasing structural damage. The lack of geotechnical investigations for residential construction in these areas and inadequate earthquake-resistant foundation designs contributed sig-

nificantly to building collapses and associated losses. Inadequate design and detailing of structural systems were widespread. This included: insufficient or absent load-carrying frames, leading to inadequate lateral load resistance; insufficient beam design in frame-column systems, resulting in excessive beam deflections and potential failure; eccentric beam connections create unbalanced forces and stress concentrations; stiffness discrepancies between floors (weak/soft floor effect) lead to uneven load distribution and potential collapse; strong beam–weak column behavior, where columns were weaker than the beams, resulting in column buckling and failure; oversized and heavy overhangs increase the seismic loads on the structure; inadequate beam–column combinations lead to insufficient load transfer; short column behavior, characterized by insufficient confinement, leads to premature failure.

The use of substandard materials and poor workmanship significantly contributed to the observed damage: low-strength concrete, reducing the structural strength and ductility; inappropriate aggregate gradation leads to poor concrete quality and reduced durability; insufficient adhesion and transverse reinforcement reduce the capacity to resist shear forces; inadequate concrete cover, leading to corrosion of reinforcing steel and reduced structural integrity; reinforcement corrosion weakens the steel and reduces its strength; use of non-ribbed (flat) reinforcement in older structures, resulting in reduced bond strength; inadequate design and construction of reinforced concrete elements, leading to stirrup opening, buckling of longitudinal bars, and core concrete disintegration; the pounding effect between adjacent structures was observed, resulting in amplified damage; out-of-plane movements in unenclosed infill and gable walls, as well as cracks and separations in partition walls, were attributed to poor workmanship and the use of weak materials.

Cities like Islahiye and Kırıkhan, despite being relatively far from the epicenter, experienced significant damage due to their proximity to fault lines. The intense ground motions generated near fault zones, including the high vertical acceleration component, exacerbated the soft story problem in cantilever beam floors, leading to structural collapse.

This research provides a technical overview of the critical factors contributing to the extensive damage observed in the 2023 Kahramanmaraş earthquakes. Understanding these factors is crucial for improving future construction practices and ensuring the resilience of buildings against seismic events.

Türkiye, situated in a highly active seismic zone, faces a constant threat from earthquakes of significant magnitude. Strengthening existing buildings to meet current earthquake codes is an urgent priority, alongside the rigorous implementation of these codes in all new construction. This study provides valuable insights for managing earthquake risk in Türkiye. Future research should prioritize the following areas: conduct an in-depth analysis of the impact of soft soil conditions and develop appropriate structural design and construction techniques tailored to these conditions; invest in research and development to enhance the seismic performance of structural systems; implement stricter control mechanisms to ensure the quality of structural materials and minimize construction errors; increase public awareness of earthquake risk through comprehensive education and outreach programs, promoting preparedness strategies.

Author Contributions: Conceptualization, E.I., F.A., A.B., Z.Ö. and R.İ.; methodology, E.I., F.A., A.B. and E.A.; validation, M.H.-N., E.I., A.B., R.İ. and E.A.; investigation, E.I., F.A., A.B. and E.A.; resources, M.H.-N., Z.Ö., D.R. and R.İ.; data curation, F.A., E.I., D.R. and E.A.; writing—original draft preparation, F.A., E.I, A.B., Z.Ö. and M.H.-N.; writing—review and editing, E.A., M.H.-N. and R.İ.; visualization, E.A. and F.A.; supervision, E.I., A.B. and F.A.; funding acquisition, M.H.-N. and D.R. All authors have read and agreed to the published version of the manuscript.

Funding: This research received no external funding.

Institutional Review Board Statement: Not applicable.

Informed Consent Statement: Not applicable.

Data Availability Statement: The data used to support the findings of this study are available from the corresponding author upon request.

Acknowledgments: The results presented in this scientific paper have been partially obtained through the research activities within the project 2023-1-HR01-KA220-HED-000165929 *Intelligent Methods for Structures, Elements and Materials* (https://im4stem.eu/en/home/ accessed on 4 June 2024) co-funded by the European Union under the program Erasmus+ KA220-HED—Cooperation partnerships in higher education.

Conflicts of Interest: The authors declare no conflicts of interest.

References

1. Türkiye Cumhuriyeti Cumhurbaşkanlığı. Available online: https://www.sbb.gov.tr/wp-content/uploads/2023/03/2023-Kahramanmaras-ve-Hatay-Depremleri-Raporu.pdf (accessed on 20 April 2023).
2. Ogunjinmi, P.D.; Park, S.S.; Kim, B.; Lee, D.E. Rapid post-earthquake structural damage assessment using convolutional neural networks and transfer learning. *Sensors* **2022**, *22*, 3471. [CrossRef] [PubMed]
3. Apostolaki, S.; Riga, E.; Pitilakis, D. Rapid damage assessment effectiveness for the 2023 Kahramanmaraş Türkiye earthquake sequence. *Int. J. Disaster Risk Reduct.* **2024**, *111*, 104691. [CrossRef]
4. Bessason, B.; Bjarnason, J.Ö. Seismic vulnerability of low-rise residential buildings based on damage data from three earthquakes (M_w6.5, 6.5 and 6.3). *Eng. Struct.* **2016**, *111*, 64–79. [CrossRef]
5. Demir, A.; Celebi, E.; Ozturk, H.; Ozcan, Z.; Ozocak, A.; Bol, E.; Sert, S.; Şahin, F.Z.; Arslan, E.; Yaman, Z.D.; et al. Destructive impact of successive high magnitude earthquakes occurred in Türkiye's Kahramanmaraş on February 6, 2023. *Bull. Earthq. Eng.* **2024**, 1–27. [CrossRef]
6. Gautam, D.; Adhikari, R.; Olafsson, S.; Rupakhety, R. Damage description, material characterization, retrofitting, and dynamic identification of a complex neoclassical monument affected by the 2015 Gorkha, Nepal earthquake. *J. Build. Eng.* **2023**, *80*, 108152. [CrossRef]
7. Bilgin, H. Effects of near-fault and far-fault ground motions on nonlinear dynamic response and seismic damage of masonry structures. *Eng. Struct.* **2024**, *300*, 117200. [CrossRef]
8. Arslan, M.H.; Korkmaz, H.H. What is to be learned from damage and failure of reinforced concrete structures during recent earthquakes in Turkey? *Eng. Fail. Anal.* **2007**, *14*, 1–22. [CrossRef]
9. Furtado, A.; Rodrigues, H.; Arêde, A.; Varum, H. A review of the performance of infilled rc structures in recent earthquakes. *Appl. Sci.* **2021**, *11*, 5889. [CrossRef]
10. Maeda, M.; Al-Washali, H.; Suzuki, K.; Takahashi, K. Damage of RC building structures due to 2011 east Japan earthquake. In Proceedings of the Structures Congress 2012, Chicago, IL, USA, 29–31 March 2012; pp. 1023–1034.
11. Kaplan, H.; Bilgin, H.; Yilmaz, S.; Binici, H.; Öztas, A. Structural damages of L'Aquila (Italy) earthquake. *Nat. Hazards Earth Syst. Sci.* **2010**, *10*, 499–507. [CrossRef]
12. Işık, E.; Işık, M.F.; Bülbül, M.A. Web based evaluation of earthquake damages for reinforced concrete buildings. *Earthq. Struct.* **2017**, *13*, 423–432. [CrossRef]
13. Kaplan, H.; Yilmaz, S.; Binici, H.; Yazar, E.; Çetinkaya, N. May 1, 2003 Turkey—Bingöl earthquake: Damage in reinforced concrete structures. *Eng. Fail. Anal.* **2004**, *11*, 279–291. [CrossRef]
14. Arslan, M.H. An evaluation of effective design parameters on earthquake performance of RC buildings using neural networks. *Eng. Struct.* **2010**, *32*, 1888–1898. [CrossRef]
15. Ruiz-Pinilla, J.G.; Adam, J.M.; Pérez-Cárcel, R.; Yuste, J.; Moragues, J.J. Learning from RC building structures damaged by the earthquake in Lorca, Spain, in 2011. *Eng. Fail. Anal.* **2016**, *68*, 76–86. [CrossRef]
16. Braga, F.; Manfredi, V.; Masi, A.; Salvatori, A.; Vona, M. Performance of non-structural elements in RC buildings during the L'Aquila, 2009 earthquake. *Bull. Earthq. Eng.* **2011**, *9*, 307–324. [CrossRef]
17. Valente, M.; Milani, G. Alternative retrofitting strategies to prevent the failure of an under-designed reinforced concrete frame. *Eng. Fail. Anal.* **2018**, *89*, 271–285. [CrossRef]
18. Masi, A.; Chiauzzi, L.; Santarsiero, G.; Manfredi, V.; Biondi, S.; Spacone, E.; Verderame, G.M. Seismic response of RC buildings during the M w 6.0 August 24, 2016 Central Italy earthquake: The Amatrice case study. *Bull. Earthq. Eng.* **2019**, *17*, 5631–5654. [CrossRef]
19. Damcı, E.; Temur, R.; Bekdaş, G.; Sayin, B. Damages and causes on the structures during the October 23, 2011 Van earthquake in Turkey. *Case Stud. Constr. Mater.* **2015**, *3*, 112–131. [CrossRef]
20. Caglar, N.; Vural, I.; Kirtel, O.; Saribiyik, A.; Sumer, Y. Structural damages observed in buildings after the January 24, 2020 Elazığ-Sivrice earthquake in Türkiye. *Case Stud. Constr. Mater.* **2023**, *18*, e01886. [CrossRef]
21. Won, J.; Shin, J. Machine learning-based approach for seismic damage prediction method of building structures considering soil-structure interaction. *Sustainability* **2021**, *13*, 4334. [CrossRef]
22. Xu, Y.; Li, Y.; Zheng, X.; Zheng, X.; Zhang, Q. Computer-vision and machine-learning-based seismic damage assessment of reinforced concrete structures. *Buildings* **2023**, *13*, 1258. [CrossRef]

23. Xiong, C.; Lu, X.; Lin, X.; Xu, Z.; Ye, L. Parameter determination and damage assessment for THA-based regional seismic damage prediction of multi-story buildings. *J. Earthq. Eng.* **2017**, *21*, 461–485. [CrossRef]
24. Tian, Y.; Ren, J.; Xu, Z.; Qi, M. A cost–benefit analysis framework for city-scale seismic retrofitting scheme of buildings. *Buildings* **2023**, *13*, 477. [CrossRef]
25. Leggieri, V.; Mastrodonato, G.; Uva, G. GIS multisource data for the seismic vulnerability assessment of buildings at the urban scale. *Buildings* **2022**, *12*, 523. [CrossRef]
26. Erduran, E. Hysteretic energy demands in multi-degree-of-freedom systems subjected to earthquakes. *Buildings* **2020**, *10*, 220. [CrossRef]
27. Gentile, R.; Galasso, C. Surrogate probabilistic seismic demand modelling of inelastic single-degree-of-freedom systems for efficient earthquake risk applications. *Earthq. Eng. Struct. Dyn.* **2022**, *51*, 492–511. [CrossRef]
28. Fajfar, P. A nonlinear analysis method for performance-based seismic design. *Earthq. Spectra* **2000**, *16*, 573–592. [CrossRef]
29. Harirchian, E.; Kumari, V.; Jadhav, K.; Rasulzade, S.; Lahmer, T.; Raj Das, R. A synthesized study based on machine learning approaches for rapid classifying earthquake damage grades to RC buildings. *Appl. Sci.* **2021**, *11*, 7540. [CrossRef]
30. Işık, E.; Avcil, F.; Arkan, E.; Büyüksaraç, A.; İzol, R.; Topalan, M. Structural damage evaluation of mosques and minarets in Adıyaman due to the 06 February 2023 Kahramanmaraş Earthquakes. *Eng. Fail. Anal.* **2023**, *151*, 107345. [CrossRef]
31. Ivanov, M.L.; Chow, W.K. Structural damage observed in reinforced concrete buildings in Adiyaman during the 2023 Turkiye Kahramanmaras Earthquakes. *Structures* **2023**, *58*, 105578. [CrossRef]
32. Kahya, V.; Genç, A.F.; Sunca, F.; Roudane, B.; Altunişik, A.C.; Yilmaz, S.; Akgül, T. Evaluation of earthquake-related damages on masonry structures due to the 6 February 2023 Kahramanmaraş-Türkiye earthquakes: A case study for Hatay Governorship Building. *Eng. Fail. Anal.* **2024**, *156*, 107855. [CrossRef]
33. Avcil, F. Investigation of precast reinforced concrete structures during the 6 February 2023 Türkiye Earthquakes. *Sustainability* **2023**, *15*, 14846. [CrossRef]
34. Arslan, M.H.; Dere, Y.; Ecemis, A.S.; Dogan, G.; Ozturk, M.; Korkmaz, S.Z. Code-based damage assessment of existing precast industrial buildings following the February 6th, 2023 Kahramanmaraş earthquakes (Pazarcık Mw 7.7 and Elbistan Mw 7.6). *J. Build. Eng.* **2024**, *86*, 108811. [CrossRef]
35. Işık, E. Structural failures of adobe buildings during the February 2023 Kahramanmaraş (Türkiye) Earthquakes. *Appl. Sci.* **2023**, *13*, 8937. [CrossRef]
36. Karasin, I.B. Comparative analysis of the 2023 Pazarcık and Elbistan earthquakes in Diyarbakır. *Buildings* **2023**, *13*, 2474. [CrossRef]
37. Zengin, B.; Aydin, F. The effect of material quality on buildings moderately and heavily damaged by the Kahramanmaraş earthquakes. *Appl. Sci.* **2023**, *13*, 10668. [CrossRef]
38. İnce, O. Structural damage assessment of reinforced concrete buildings in Adıyaman after Kahramanmaraş (Türkiye) Earthquakes on 6 February 2023. *Eng. Fail. Anal.* **2023**, *156*, 107799. [CrossRef]
39. Ozturk, M.; Arslan, M.H.; Dogan, G.; Ecemis, A.S.; Arslan, H.D. School buildings performance in 7.7 Mw and 7.6 Mw catastrophic earthquakes in southeast of Turkey. *J. Build. Eng.* **2023**, *79*, 107810. [CrossRef]
40. Ozturk, M.; Arslan, M.H.; Korkmaz, H.H. Effect on RC buildings of 6 February 2023 Turkey earthquake doublets and new doctrines for seismic design. *Eng. Fail. Anal.* **2023**, *153*, 107521. [CrossRef]
41. Akar, F.; Işık, E.; Avcil, F.; Büyüksaraç, A.; Arkan, E.; İzol, R. Geotechnical and structural damages caused by the 2023 Kahramanmaraş Earthquakes in Gölbaşı (Adıyaman). *Appl. Sci.* **2024**, *14*, 2165. [CrossRef]
42. Binici, B.; Yakut, A.; Kadas, K.; Demirel, O.; Akpinar, U.; Canbolat, A.; Yurtseven, F.; Oztaskin, O.; Aktas, S.; Canbay, E. Performance of RC buildings after Kahramanmaraş earthquakes: Lessons toward performance based design. *Earthq. Eng. Eng. Vib.* **2023**, *22*, 883–894. [CrossRef]
43. Işık, E.; Avcil, F.; İzol, R.; Büyüksaraç, A.; Bilgin, H.; Harirchian, E.; Arkan, E. Field reconnaissance and earthquake vulnerability of the RC buildings in Adıyaman during 2023 Türkiye Earthquakes. *Appl. Sci.* **2024**, *14*, 2860. [CrossRef]
44. Cetin, K.O.; Soylemez, B.; Guzel, H.; Cakir, E. Soil liquefaction sites following the February 6, 2023, Kahramanmaraş-Türkiye earthquake sequence. *Bull. Earthq. Eng.* **2024**, 1–24. [CrossRef]
45. Kocaman, İ.; Mercimek, Ö.; Gürbüz, M.; Erbaş, Y.; Anıl, Ö. The effect of Kahramanmaraş earthquakes on historical Malatya Yeni Mosque. *Eng. Fail. Anal.* **2024**, *161*, 108310. [CrossRef]
46. Kocaman, İ. The effect of the Kahramanmaraş earthquakes (Mw 7.7 and Mw 7.6) on historical masonry mosques and minarets. *Eng. Fail. Anal.* **2023**, *149*, 107225. [CrossRef]
47. Mercimek, Ö. Seismic failure modes of masonry structures exposed to Kahramanmaraş earthquakes (Mw 7.7 and 7.6) on February 6, 2023. *Eng. Fail. Anal.* **2023**, *151*, 107422. [CrossRef]
48. Tunç, G.; Mertol, H.C.; Akış, T. Lessons learned from four recent Turkish earthquakes: Sivrice-Elazığ, Aegean Sea, and Dual Kahramanmaraş. *Nat. Hazards* **2024**. [CrossRef]
49. Ersoz, A.B.; Pekcan, O.; Altun, M.; Teke, T.; Aydogmus, O. Utilizing digital technologies for rapid damage assessment and reconnaissance: The February 6, 2023 Kahramanmaraş-Türkiye earthquakes (Mw 7.7 and Mw 7.6). *Bull. Earthq. Eng.* **2024**, 1–19. [CrossRef]

50. Kazaz, İ.; Avşar, Ö.; Dilsiz, A. Importance of building inspection on the seismic response of a severely damaged RC structure during the February 6, 2023 Kahramanmaraş earthquake sequence. *Eng. Fail. Anal.* **2024**, *162*, 108410. [CrossRef]
51. Nemutlu, Ö.F.; Sarı, A.; Balun, B. 06 Şubat 2023 Kahramanmaraş Depremlerinde (Mw 7.7-Mw 7.6) meydana gelen gerçek can kayıpları ve yapısal hasar değerlerinin tahmin edilen değerler ile karşılaştırılması. *Afyon Kocatepe Üniversitesi Fen Mühendislik Bilim. Derg.* **2023**, *23*, 1222–1234. [CrossRef]
52. Ergin, K.; Guglu, U.; Uz, Z. A catalogue of earthquakes of Turkey and surrounding area (11 A.D. to 1964 A.D.). *Maden Fakültesi Arz Fiziği Enstitüsü Yayin. Istanb.* **1967**, *24*, 169.
53. Över, S.; Ünlügenç, U.C.; Bellier, O. Quaternary stress regime change in the Hatay region (SE Turkey). *Geophy. J. Int.* **2002**, *148*, 649–662. [CrossRef]
54. Emre, Ö.; Duman, T.Y.; Özalp, S.; Şaroğlu, F.; Olgun, Ş.; Elmacı, H.; Çan, T. Active fault database of Turkey. *Bull. Earthq. Eng.* **2018**, *16*, 3229–3275. [CrossRef]
55. Kurnaz, T.F.; Ince, Y. Evaluation of seismic hazard with probabilistic approach for Antakya Province (Turkey). *J. Earth Syst. Sci.* **2020**, *129*, 172. [CrossRef]
56. Willis, B. Earthquakes in the Holy Land. *Bull. Seismol. Soc. Am.* **1928**, *18*, 73–103. [CrossRef]
57. Sieberg, A. Erdbebengeographie. *Handb. Geophys.* **1932**, *4*, 708–744.
58. Ambraseys, N.N. Some characteristic features of the Anatolian fault zone. *Tectonophysics* **1970**, *9*, 143–165. [CrossRef]
59. Poirier, J.P.; Taher, M.A. Historical seismicity in the near and Middle East, North Africa, and Spain from Arabic documents (VIIth-XVIIIth century). *Bull. Seismol. Soc. Am.* **1980**, *70*, 2185–2201. [CrossRef]
60. Soysal, H.; Sipahioglu, S.; Kolcak, D.; Altinok, Y. *Türkiye ve Çevresinin Tarihsel Deprem Katalogu*; TUBITAK Proje no. TBAG 341 Istanbul 86; TUBITAK: Ankara, Türkiye, 1981. (In Turkish)
61. Ambraseys, N.N.; Barazangi, M. The 1759 earthquake in the Bekaa Valley: Implications for earthquake hazard assessment in the Eastern Mediterranean region. *J. Geophys. Res. Solid Earth* **1989**, *B4*, 4007–4013. [CrossRef]
62. Ambraseys, N.N.; Jackson, J.A. Faulting associated with historical and recent earthquakes in the Eastern Mediterranean region. *Geophys. J. Int.* **1998**, *133*, 390–406. [CrossRef]
63. Çetin, H.; Güneyli, H.; Mayer, L. Paleoseismology of the Palu Lake Hazar Segment of the East Anatolian Fault Zone, Turkey. *Tectonophysics* **2003**, *374*, 163–197. [CrossRef]
64. Alkan, H.; Büyüksaraç, A.; Bektaş, Ö.; Işık, E. Coulomb stress change before and after 24.01. 2020 Sivrice (Elazığ) Earthquake (Mw = 6.8) on the East Anatolian Fault Zone. *Arab. J. Geosci.* **2021**, *14*, 2648. [CrossRef]
65. AFAD. 2024. Available online: https://tdth.afad.gov.tr (accessed on 15 May 2024).
66. Aktug, B.A.; Ozener, H.; Dogru, A.; Sabuncu, A.; Turgut, B.; Halicioglu, K.; Yilmaz, O.; Havazli, E. Slip rates and seismic potential on the East Anatolian Fault System using an improved GPS velocity field. *J. Geodyn.* **2016**, *94–95*, 1–2. [CrossRef]
67. Reilinger, R.; McClusky, S.; Vernant, P.; Lawrence, S.; Ergintav, S.; Cakmak, R.; Ozener, H.; Kadirov, F.; Guliev, I.; Stepanyan, R.; et al. GPS constraints on continental deformation in the Africa-Arabia-Eurasia continental collision zone and implications for the dynamics of plate interactions. *J. Geophys. Res. Solid Earth* **2006**, *111*, B05411. [CrossRef]
68. McClusky, S.; Balassanian, S.; Barka, A.; Demir, C.; Ergintav, S.; Georgiev, I.; Gurkan, O.; Hamburger, M.; Hurst, K.; Kahle, H.; et al. Global positioning system constraints on plate kinematics and dynamics in the eastern mediterranean and Caucasus. *J. Gephys. Res.* **2000**, *105*, 5695–5719. [CrossRef]
69. Mahmoud, Y.; Masson, F.; Meghraoui, M.; Cakir, Z.; Alchalbi, A.; Yavasoglu, H.; Yönlü, O.; Daoud, M.; Ergintav, S.; Inan, S. Kinematic study at the junction of the East Anatolian fault and the Dead Sea fault from GPS measurements. *J. Geodyn.* **2013**, *67*, 30–39. [CrossRef]
70. Altunel, E.; Meghraoui, M.; Karabacak, V.; Akyüz, S.H.; Ferry, M.; Yalçıner, Ç.; Munschy, M. Archaeological sites (tell and road) offset by the Dead Sea Fault in the Amik Basin, southern Turkey. *Geophys. J. Int.* **2009**, *179*, 1313–1329. [CrossRef]
71. Westaway, R. Kinematic consistency between the Dead Sea Fault Zone and the Neogene and Quaternary left-lateral faulting in SE Turkey. *Tectonophysics* **2004**, *391*, 203–237. [CrossRef]
72. Over, S.; Kavak, K.Ş.; Bellier, O.; Özden, S. Is the Amik Basin (SE Turkey) a triple-junction area? Analyses of SPOT XS imagery and seismicity. *Int. J. Remote Sens.* **2004**, *25*, 3857–3872. [CrossRef]
73. Duman, T.Y.; Emre, Ö. The East Anatolian Fault: Geometry, segmentation and jog characteristics. *Geol. Soc. Lond. Spec. Publ.* **2013**, *372*, 495–529. [CrossRef]
74. Nalbant, S.S.; McCloskey, J.; Steacy, S.; Barka, A.A. Stress accumulation and increased seismic risk in eastern Turkey. *Earth Planet. Sci. Lett.* **2022**, *195*, 291–298. [CrossRef]
75. AFAD. *06 Şubat 2023 Pazarcık-Elbistan Kahramanmaraş (Mw: 7.7–Mw: 7.6) Depremleri Raporu*; Deprem ve Risk Azaltma Genel Müdürlüğü Deprem Dairesi Başkanlığı: Ankara, Türkiye, 2023.
76. Büyüksaraç, A.; Bektaş, Ö.; Alkan, H. Fault modeling around southern Anatolia using the aftershock sequence of the Kahramanmaraş earthquakes (M_w = 7.7 and M_w = 7.6) and an interpretation of potential field data. *Acta Geophys.* **2024**, *72*, 2985–2996. [CrossRef]
77. TBEC. *Turkish Building Earthquake Code*; T.C. Resmi Gazete: Ankara, Turkey, 2018.

78. Cagatay, I.H.; Beklen, C.; Mosalam, K.M. Investigation of short column effect of RC buildings: Failure and prevention. *Comput. Concr.* **2010**, *7*, 523–532. [CrossRef]
79. TEC. *Turkish Earthquake Code*; Ministry of Public Works and Settlement: Ankara, Turkey, 2007.